HUMAN GENE THERAPY 23:345–355 (April 2012)
© Mary Ann Liebert, Inc.
DOI: 10.1089/hum.2011.115

Research Articles

Dextran and Protamine-Based Solid Lipid Nanoparticles as Potential Vectors for the Treatment of X-Linked Juvenile Retinoschisis

Diego Delgado,[1] Ana del Pozo-Rodríguez,[1] Maria Ángeles Solinís,[1] Marcelino Avilés-Triqueros,[2] Bernhard H.F. Weber,[3] Eduardo Fernández,[2] and Alicia R. Gascón[1]

Abstract

The goal of the present study was to analyze the potential application of nonviral vectors based on solid lipid nanoparticles (SLN) for the treatment of ocular diseases by gene therapy, specifically X-linked juvenile retinoschisis (XLRS). Vectors were prepared with SLN, dextran, protamine, and a plasmid (pCMS-EGFP or pCEP4-RS1). Formulations were characterized and the *in vitro* transfection capacity as well as the cellular uptake and the intracellular trafficking were studied in ARPE-19 cells. Formulations were also tested *in vivo* in Wistar rat eyes, and the efficacy was studied by monitoring the expression of enhanced green fluorescent protein (EGFP) after intravitreal, subretinal, and topical administration. The presence of dextran and protamine in the SLN improved greatly the expression of retinoschisin and EGFP in ARPE-19 cells. The nuclear localization signals of protamine, its ability to protect the DNA, and a shift in the entry mechanism from caveola-mediated to clathrin-mediated endocytosis promoted by the dextran, justify the increase in transfection. After ocular administration of the dextran–protamine–DNA–SLN complex to rat eyes, we detected the expression of EGFP in various types of cells depending on the administration route. Our vectors were also able to transfect corneal cells after topical application. We have demonstrated the potential usefulness of our nonviral vectors loaded with XLRS1 plasmid and provided evidence for their potential application for the management or treatment of degenerative retinal disorders as well as ocular surface diseases.

Introduction

In spite of important advances in the treatment and prevention of eye diseases, many causes of vision loss still do not have a cure, and even with the best medical treatment many persons must live with impaired vision. Gene therapy is considered a hopeful option for the treatment of hereditary but also acquired eye diseases. Its clinical potential was demonstrated by major improvements of visual function in the first clinical trials with patients with Leber's congenital amaurosis (Bainbridge *et al*., 2008; Maguire *et al*., 2009). In general, the eye is an ideal target for gene therapy because of its exceptional attributes such as ease of access as well as suitable and highly sensitive methods for monitoring even minor changes of visual function. The well-defined anatomy and immunoprivilege of the eye are also important advantages for gene therapy (Liu *et al*., 2007). The small dimensions of this organ make unnecessary a high concentration of product to achieve therapeutic effects, while the diffusion from the eye into the circulation is limited (Bloquel *et al*., 2006; Naik *et al*., 2009).

Inherited retinal degenerations have a prevalence of 1:4,000, with a progressive and often untreatable course (Hamel, 2006). For example, X-linked juvenile retinoschisis (XLRS) is a common source of male juvenile blindness with a prevalence of 1:5,000 to 1:25,000 (Mooy *et al*., 2002). The application of gene replacement therapy in XLRS has been considered a promising therapeutic approach for this disease. Proof of concept was provided by several groups using viral delivery systems in retinoschisin-deficient mice (Min *et al*., 2005; Janssen *et al*., 2008). However, these vectors present important limitations due to immunogenicity and

[1]Pharmacokinetics, Nanotechnology and Gene Therapy Group Laboratory of Pharmacy and Pharmaceutical Technology, Pharmacy Faculty, University of the Basque Country UPV/EHU, 01006 Vitoria-Gasteiz, Spain.
[2]Bioengineering Institute, Miguel Hernández University, 03202 Elche, Spain.
[3]Institute of Human Genetics, University of Regensburg, D-93053 Regensburg, Germany.

oncogenicity (Kumar-Singh, 2008). Moreover, there is evidence for the potential persistence of viral vectors in brain after intravitreal injection (Provost *et al*., 2005). These drawbacks have motivated the development of nonviral systems.

In preceding studies we have developed nonviral vectors composed of cationic lipids, more precisely solid lipid nanoparticles (SLNs) (del Pozo-Rodríguez *et al*., 2009; Delgado *et al*., 2011; Gascón *et al*., 2011). These SLNs have shown the capacity to transfect *in vitro* retinal pigment epithelium (RPE) cells, used as a model for inherited retinal diseases (del Pozo-Rodríguez *et al*., 2008). In an effort to expand our previous work, the goal of the present work was to study the potential application of solid lipid nanoparticle-based nonviral vectors for the treatment of ocular diseases, specifically XLRS. With this goal in mind, we measured the protein produced (green fluorescence protein or retinoschisin) after *in vitro* transfection of retinal cells (ARPE-19 cell line) with the vectors containing the plasmids that codify those proteins. We also monitored the internalization of our vectors into the cells, their trafficking inside cytosol, and the transport of plasmids to the nucleus in retinal cells. After the *in vitro* characterization, the vectors were administered to rat eyes and the efficacy was studied by monitoring the expressed enhanced green fluorescent protein.

Materials and Methods

Production of vectors

Preparation of SLN. Nanoparticles were prepared by a solvent emulsification–evaporation technique previously described by del Pozo-Rodríguez and colleagues (2007). Briefly, a solution of Precirol ATO 5 (Gattefossé, Madrid, Spain) in dichloromethane (Panreac, Barcelona, Spain) was emulsified by sonication (Branson sonifier 250; Branson Ultrasonics/Emerson, Danbury, CT) in an aqueous phase containing 0.4% (w/v) DOTAP (trimethylammoniumpropane chloride salt; Avanti Polar Lipids, Alabaster, AL) and 0.1% (w/v) Tween 80 (Vencaser, Bilbao, Spain). After evaporation of the organic solvent the SLN suspension was formed. The suspension was then washed by passage through 100,000 molecular weight cutoff (MWCO) Amicon Ultra centrifugal filters (3,000 rpm, 20 min, three times; Millipore, Billerica, MA).

Preparation of dextran–protamine–DNA complexes. First, an aqueous solution of dextran (number average molecular weight [M_n] 3260; Sigma-Aldrich, St. Louis, MO) was mixed with an aqueous solution of protamine sulfate grade X (Sigma-Aldrich) to form dextran–protamine complexes at weight-to-weight ratios of 0.5:2, 1:2, and 2:2. The plasmid was then bound to the dextran–protamine complexes to set dextran–protamine–DNA ratios of 0.5:2:1, 1:2:1, and 2:2:1 (w/w/w). After dilution in Milli-Q water, complexes were subjected to electrophoresis on an agarose gel (0.6% agarose, 1% ethidium bromide), and DNA bands were observed with a UVIdoc D55-LCD-20M Auto transilluminator (UVItec, Cambridge, UK).

Preparation of vectors. To obtain DNA–SLN vectors, pCMS-EGFP plasmid was mixed with the SLN suspension at a DOTAP-to-DNA ratio of 5:1 (w/w). This plasmid (Clontech, Palo Alto, CA) encodes enhanced green fluorescent protein (EGFP). Regarding pCEP4-RS1 plasmid, DOTAP-to-DNA ratios of 5:1 and 6:1 (w/w) were compared. This second plasmid, which encodes retinoschisin protein, was prepared at the Institute of Human Genetics of the University of Regensburg (Regensburg, Germany).

To obtain dextran–protamine–DNA–SLN vectors, dextran–protamine–DNA complexes were mixed with SLN suspension for 30 min, after which dextran–protamine–DNA complexes were adsorbed on the nanoparticle surface.

Measurements of size (photon correlation spectroscopy; PCS) and ζ potential (laser Doppler velocimetry; LDV) of SLNs and of DNA–SLN and dextran–protamine–DNA–SLN (1:2:1:5) vectors were carried out with a Malvern Zetasizer 3000 (Malvern Instruments, Worcestershire, UK).

DNase protection study and DNA plasmid release study

DNase I (deoxyribonuclease I; Sigma-Aldrich) was added to DNA–SLN and dextran–protamine–DNA–SLN vectors (1 U of DNase I per 2.5 μg of DNA), and incubated at 37°C for 30 min. To release plasmid from the vectors, SDS (lauryl sulfate sodium; Sigma-Aldrich) was added to a final concentration of 1%. The integrity of the DNA in each sample was compared with that of a control, untreated DNA, by means of electrophoresis on agarose gels (see Preparation of Dextran–Protamine–DNA Complexes, above).

Cell cultures

Retinal pigment epithelial cells (ARPE-19), from the American Type Culture Collection (ATCC, Manassas, VA), were used for *in vitro* studies. ARPE-19 cells were maintained in Dulbecco's modified Eagle's medium–Ham's nutrient mixture F12 (1:1) (Gibco DMEM/F12; Life Technologies, Carlsbad, CA) containing 1% Normocin antibiotic (InvivoGen, San Diego, CA) and 10% fetal bovine serum (Life Technologies). Cells were cultured in 5% CO_2 at 37°C and subcultured every 2–3 days.

In vitro *transfection assays*

Vectors containing pCMS-EGFP plasmid. For transfection studies with pCMS-EGFP plasmid, ARPE-19 cells were cultured on 12-well plates (30,000 cells per well) and treated as previously described (del Pozo-Rodríguez *et al*., 2008). Briefly, vectors containing 2.5 μg of DNA were added to each well, and transfection efficacy was measured 12 hr, 24 hr, 48 hr, 72 hr, and 1 week after addition of vectors.

Transfection evaluation by flow cytometry. At the time points indicated, cells were washed with phosphate-buffered saline (PBS), detached, and centrifuged at 1500 × *g*. After resuspension in PBS, cells were directly introduced into a FACSCalibur flow cytometer (BD Biosciences, San Jose, CA) to measure the fluorescence of EGFP (FL1, 525 nm). Cell viability was assessed with a Via-Probe kit (BD Biosciences), which allows exclusion of dead cells by measuring fluorescence at 650 nm (FL3). From each sample, 10,000 events were collected.

Vectors containing pCEP4-RS1 plasmid. *Immunochemical detection of retinoschisin.* ARPE-19 cells were seeded on coverslips and transfected with plasmid pCEP4-RS1 as described

in Vectors Containing pCMS-EGFP Plasmid (above). Seventy-two hours after addition of vectors, cells were permeabilized and blocked with PBS containing 0.2% Triton X-100 (Sigma-Aldrich) and 10% normal goat serum (Sigma-Aldrich) for 20 min and labeled overnight with monoclonal RS1-3R10 antibody (produced at the Institute of Human Genetics of the University of Regensburg; Molday *et al.*, 2001) diluted in PBS containing 0.1% Triton X-100 and 2.5% normal goat serum. Samples were rinsed in PBS and labeled for 1 hr with Alexa Fluor 488-conjugated goat anti-rabbit IgG (Life Technologies). Cells were also treated with 4', 6-diamidino-2-phenylindole dihydrochloride (DAPI; Sigma-Aldrich) nuclear stain and, after mounting with Fluoromount-G (SouthernBiotech, Birmingham, AL), images were captured with an inverted microscope equipped with an attachment for fluorescence observation (Eclipse TE2000-S; Nikon Instruments, Melville, NY).

Quantification of secreted retinoschisin. ARPE-19 cells were treated with plasmid pCEP4-RS1 as described in the transfection procedure in Vectors Containing pCMS-EGFP Plasmid (above). Seventy-two hours after addition of vectors, retinoschisin produced by the cells was quantified with an ELISA kit (Uscn Life Science, Wuhan, China).

Cellular uptake of nonviral vectors

To monitor the cellular uptake of nonviral vectors, the fluorescent dye Nile red ($\lambda = 590$ nm; Sigma-Aldrich) was incorporated into the SLNs according to a previously reported method (del Pozo-Rodríguez *et al.*, 2008). Two hours after the addition of vectors, cells were washed three times with PBS before detachment. Cells incorporating either DNA–SLN or dextran–protamine–DNA–SLN vectors were quantified by flow cytometry (FL3, 650 nm). For each sample, 10,000 events were collected.

Colocalization assay

Alexa Fluor 488–cholera toxin and Alexa Fluor 488–transferrin were used as markers of caveola/raft-mediated and clathrin-mediated endocytosis, respectively. The colocalization of these molecules with Nile red-labeled vectors was studied by confocal laser scanning microscopy (CLSM) as described in a previous paper by del Pozo-Rodríguez and colleagues (2008). In brief, cells seeded in coverslips were coincubated with the vectors and either Alexa Fluor 488–cholera toxin or Alexa Fluor 488–transferrin. Once cells were mounted with Fluoromount-G, images were obtained with a Fluoview FV500 confocal microscope (Olympus, Tokyo, Japan), by the General Service of Analytical Microscopy and High Resolution in Biomedicine of the University of the Basque Country UPV/EHU, using sequential acquisition to avoid overlapping of fluorescent emission spectra.

The Manders overlap coefficient (R) was calculated to estimate colocalization degree (Zinchuk and Zinchuk, 2008). Overlap of the signals was considered when $0.6 \leq R \leq 1.0$.

In vivo *study in rats*

The animal experiments were done according to the European Union regulations for the use of animals in research; the Association for Research in Vision and Ophthalmology (ARVO) statement for the use of animals in ophthalmic and vision research; and the guidelines published by the Institute for Laboratory Animal Research (*Guide for the Care and Use of Laboratory Animals*). The animal protocol was approved by the Institutional Animal Care and Use Committee of the University Miguel Hernández (Elche, Spain). Wistar rats (Harlan Interfauna Ibérica, Barcelona, Spain) weighing 100–150 g (5 weeks of age) were used in the experiment.

The surgical procedures used for the transplantation and administration of vectors without plasmid (control) or with dextran–protamine–DNA–SLN complexes in the retina have been described elsewhere (Nour *et al.*, 2003; Jiang *et al.*, 2007). Briefly, rats kept at a 12-hr light–dark cycle were anesthetized with an intraperitoneal injection of a mixture of ketamine (Ketalar, 70 mg/kg; Pfizer, Alcobendas, Madrid, Spain) and xylazine (Rompun, 10 mg/kg; Bayer, Kiel, Germany) in 0.1 ml of saline. Next, their pupils were dilated with one drop of 1% tropicamide solution (Colircusi Tropicamida; Alcon, Barcelona, Spain) and the cornea was anesthetized with a drop of 4% oxybuprocaine and 1% tetracaine (Colircusi Anestesico Doble; Alcon).

Intravitreous administration. Intravitreal injection was performed under general anesthesia, using an operating microscope (OPMI; Zeiss, Oberkochen, Germany). A 30-gauge hypodermic needle was used to perforate the sclera 1.5 mm behind the limbus. The hypodermic needle was then withdrawn, and a 33-gauge blunt needle (Hamilton, Reno, NV) was inserted through the hole and advanced into the anterior chamber, avoiding the iris and lens. The needle was angled to point slightly nasally and guided posteriorly into the eye. The lens was displaced medially as the needle was advanced through the vitreous cavity toward the retinal surface. Once the tip of the needle had reached the desired location, 3 µl of dextran–protamine–DNA–SLN solution (0.09 µg of plasmid DNA) was injected into the vitreous cavity of the left eye ($n = 3$). Care was taken not to damage the lens. After intraocular injections, the needle was held in place for 1 min and withdrawn slowly. In addition, paracentesis was simultaneously performed to relieve pressure and thereby prevent reflux. The right eye was kept as control. After the injection, one drop of ofloxacin ophthalmic solution (Exocin; Allergan, Barcelona, Spain) was applied to both eyes. Last, the retinas were examined funduscopically with a stereomicroscope (Leitz, Wetzlar, Germany) after the injection, and animals with retinal bleeding or lens injury after the injection procedure were excluded from the study.

Subretinal administration. The procedure for subretinal administration was similar to that for intravitreous injection and was performed under general anesthesia with an operating microscope (OPMI; Zeiss). A 30-gauge hypodermic needle was used to perforate the sclera. With a 30-gauge needle (Hamilton), dextran–protamine–DNA–SLN was injected into the superior subretinal space of the left eye ($n = 3$). The needle passed through the sclera and then 1–2 µl of dextran–protamine–DNA–SLN complexes was injected (0.03–0.06 µg of plasmid DNA). After the injection, one drop of ofloxacin ophthalmic solution (Exocin; Allergan) was applied as antibiotic to the eye. The retinas were examined funduscopically with a stereomicroscope (Leitz) after the injection, and eyes showing massive subretinal hemorrhage, vitreous hemorrhage, or large retinal detachments were excluded.

Topical administration. For the *in vivo* study, rat corneas ($n=3$) were treated with dextran–protamine–DNA–SLN complexes by triple instillation of drops (10 µl each instillation, 3 µg of plasmid DNA). To avoid possible interactions, neither antibiotics nor any other ophthalmic solutions were used after the administration.

Microscopy analysis. Animals were killed with an intraperitoneal overdose of sodium pentobarbital. The eyes were enucleated and fixed for 60 min at room temperature in 4% paraformaldehyde in 0.1 *M* PBS. The eyes were then washed with PBS, the corneas were excised, and the retinas were isolated.

Flat-mounted preparations of the retina, including the RPE layer, and cornea were examined and photographed by fluorescence microscopy (model AX70; Olympus) or by confocal microscopy (TCS SP5 II; Leica Microsystems, Wetzlar, Germany). In addition, some samples were cryoprotected at room temperature in phosphate buffer (PB) containing 12.5% sucrose (for 45 min) or in PB containing 25% sucrose (for at least 1 hr). The tissue was then embedded in Tissue Tek O.C.T. compound (Sakura Finetek Europe, Alphen aan den Rijn, The Netherlands) and frozen on dry ice. Vertical 20-µm-thick cryosections were prepared and placed on Superfrost Plus slides (Menzel-Gläser, Braunschweig, Germany). For staining cell nuclei, cryosections were incubated for 20 min in Hoechst 33342 dye (diluted 1:10,000; Sigma-Aldrich). Sections were then rinsed in PBS, mounted with VECTASHIELD (Vector Laboratories, Burlingame, CA), and stored at 4°C. The sections were photographed with the help of a fluorescence microscope (model AX70; Olympus) or analyzed by confocal microscopy (TCS SP5 II; Leica Microsystems).

Evaluation of gene expression. To evaluate transfection efficiency *in vivo*, the expression of green fluorescent protein was observed 72 hr after intravitreal and subretinal injections, and 72 and 120 hr after topical instillation in corneas.

Transfection controls were performed with vectors without pCMS-EGFP plasmid.

Statistical analysis

Results are reported as mean values. Error bars in the figures represent the standard deviation (SD). Comparisons were performed by analysis of variance (ANOVA) and Student *t* test, after assessing the normal distribution of the samples and the homogeneity of variances. Data were considered statistically significant when p values were less than 0.05. Statistical analysis was performed with SPSS 17.0 (SPSS, Chicago, IL).

Results

Production of vectors

Dextran, protamine, and pCMS-EGFP plasmid were combined at ratios of 0.5:2:1, 1:2:1, and 2:2:1, respectively, and the resulting complexes were subjected to electrophoresis on an agarose gel (Fig. 1A). Results indicated that DNA was fully bound in the complexes at all indicated dextran and protamine proportions.

The DNA–SLN vector and the dextran–protamine–DNA–SLN vector showed particle sizes between 200 and 270 nm (Fig. 2), and a surface charge of about +35 mV, irrespective of the plasmid used, that is, pCMS-EGFP or pCEP4-RS1. No differences in particle size and ζ potential between DNA–SLN and dextran–protamine–DNA–SLN formulations were detected ($p>0.05$).

In vitro *resistance to DNase and SDS-induced release of plasmids from vectors*

Plasmid protection in DNA–SLN and dextran–protamine–DNA–SLN vectors and release from them were studied by agarose gel electrophoresis after treatment with DNase I (Fig. 1B) and SDS (Fig. 1C). Figures 1B and 1C show the ability of both vectors to preserve and release the pCMS-EGFP plasmid they transport. When vectors were prepared with pCEP4-RS1 plasmid, a DNA-to-SLN ratio of 1:6 showed a higher protection capacity than the 1:5 ratio, without hampering plasmid release (Fig. 3).

Transfection and cell viability studies in ARPE-19 cells

Plasmid pCMS-EGFP. Vectors prepared at various dextran–protamine ratios were assayed to study their

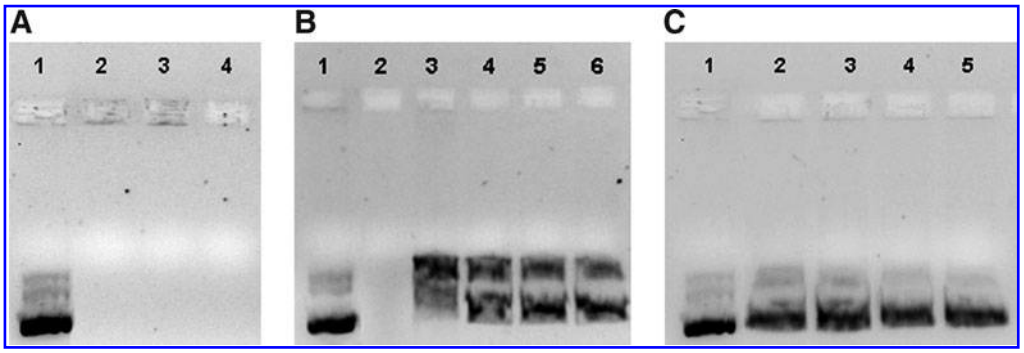

FIG. 1. **(A)** Binding efficiency of pCMS-EGFP plasmid at various dextran–protamine–DNA ratios (w/w/w) studied by agarose gel electrophoresis. Lane 1, free DNA; lane 2, 0.5:2:1; lane 3, 1:2:1; lane 4, 2:2:1. **(B)** Protection of DNA by dextran–protamine–DNA–SLN vectors from DNase digestion at various dextran–protamine–DNA–SLN ratios (w/w/w/w). Vectors were treated with DNase I. Lane 1, free DNA; lane 2, DNase-treated free DNA; lane 3, DNA–SLN vectors; lane 4, 0.5:2:1:5; lane 5, 1:2:1:5; lane 6, 2:2:1:5. **(C)** Release of DNA, after DNase digestion, by dextran–protamine–DNA–SLN vectors at various dextran–protamine–DNA–SLN ratios (w/w/w/w). Vectors were treated with SDS. Lane 1, free DNA; lane 2, DNA–SLN; lane 3, 0.5:2:1:5; lane 4, 1:2:1:5; lane 5, 2:2:1:5.

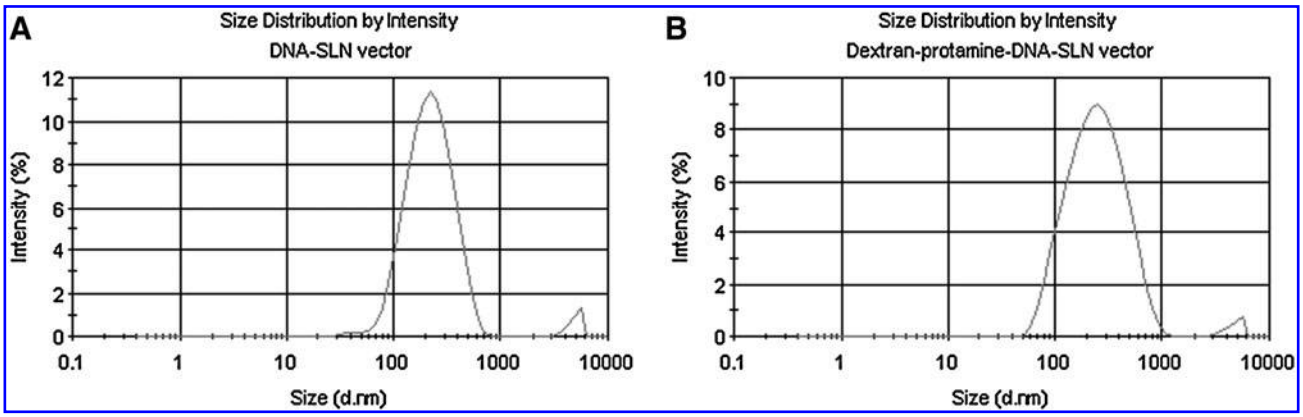

FIG. 2. Size distribution of the DNA–SLN vector **(A)** and dextran–protamine–DNA–SLN vector **(B)**.

capacity for cell transfection in ARPE-19 cells. We previously checked that dextran–protamine–DNA complexes were not able to transfect cells. As observed in Fig. 4A (columns), transfection levels at 72 hr were maximum (44% EGFP-positive cells) when dextran–protamine–DNA–SLN vectors were used at a 1:2:1:5 ratio, whereas DNA–SLN vectors resulted in only 7% transfected cells ($p < 0.01$). Cell viability (line in Fig. 4A) obtained with the vectors containing dextran and protamine was significantly higher than viability obtained with the DNA–SLN vector ($p < 0.01$).

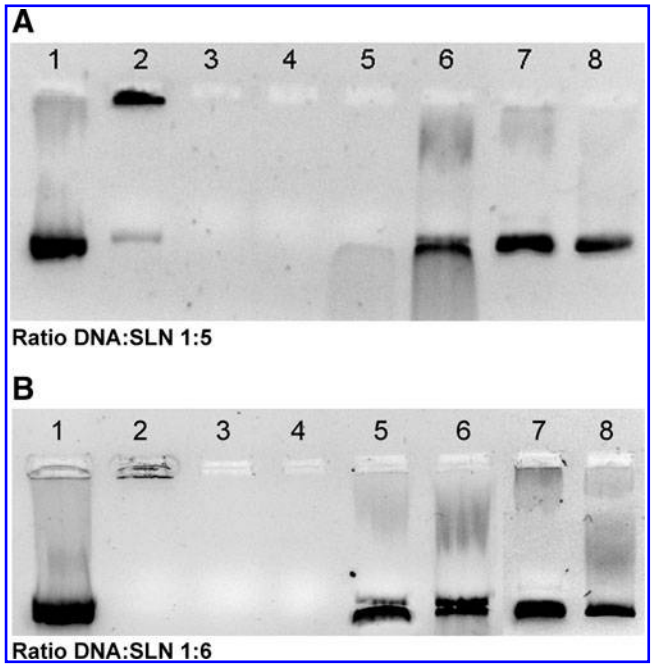

FIG. 3. Protection of pCEP4-RS1 from DNase I digestion, binding efficiency, and ability to release plasmid from the complexes, visualized by agarose gel electrophoresis. **(A)** Lane 1, free DNA; lane 2, DNA–SLN; lane 3, dextran–protamine–DNA–SLN; lane 4, free DNA with DNase; lane 5, DNA–SLN with DNase; lane 6, dextran–protamine–DNA–SLN with DNase; lane 7, DNA–SLN with SDS; lane 8, dextran–protamine–DNA–SLN with SDS. The SLN-to-DNA ratio, expressed as the ratio of DOTAP to DNA (w/w), was fixed at 5:1; dextran–protamine solution was prepared at a ratio (w/w) of 1:2. **(B)** Lane 1, free DNA; lane 2, DNA–SLN; lane 3, dextran–protamine–DNA–SLN; lane 4, free DNA with DNase; lane 5, DNA–SLN with DNase; lane 6, dextran–protamine–DNA–SLN with DNase; lane 7, DNA–SLN with SDS; lane 8, dextran–protamine–DNA–SLN with SDS. The SLN-to-DNA ratio, expressed as the ratio of DOTAP to DNA (w/w), was fixed at 6:1; dextran–protamine solution was prepared at a ratio (w/w) of 1:2.

Subsequently, the transfection capacity of the most effective formulation (dextran–protamine–DNA–SLN at a 1:2:1:5 ratio) and control formulation (DNA–SLN at a 1:5 ratio) was studied over time (Fig. 4B). Transfection was detected from 24 hr and progressively increased with both formulations, but at every time point the dextran–protamine–DNA–SLN formulation showed higher efficacy ($p < 0.01$).

Plasmid pCEP4-RS1. Retinoschisin present in cytoplasm 72 hr after transfection of ARPE-19 cells with pCEP4-RS1 plasmid was detected by immunochemistry. Figure 5 shows the protein expressed (green) after treating cells with DNA–SLN vector (Fig. 5B) and dextran–protamine–DNA–SLN vector (Fig. 5A). Both vectors were able to transfect pCEP4-RS1. Cell nuclei were labeled with DAPI (blue).

Figure 5C show the levels of retinoschisin secreted by ARPE-19 cells 72 hr posttransfection. The presence of dextran and protamine in the nanoparticles induced significantly higher expression of retinoschisin ($p < 0.01$). These results are consistent with those obtained with pCMS-EGFP.

Cellular uptake of nonviral vectors

No differences in cell uptake were detected between the two formulations (DNA–SLN and dextran–protamine–DNA–SLN vectors). The presence of dextran and protamine in the vectors did not modify their capacity to enter ARPE-19 cells (Fig. 6).

Colocalization assay

The uptake mechanism of the two vectors in ARPE-19 cells was studied by CLSM. Colocalization studies were carried out with Alexa Fluor 488-labeled transferrin and cholera toxin, the markers of endocytosis via clathrin and via caveolae, respectively (Fig. 7). Both markers were found in the cells, suggesting that the two mechanisms of endocytosis are present in this cell line. The most significant finding was higher colocalization with transferrin when the vector

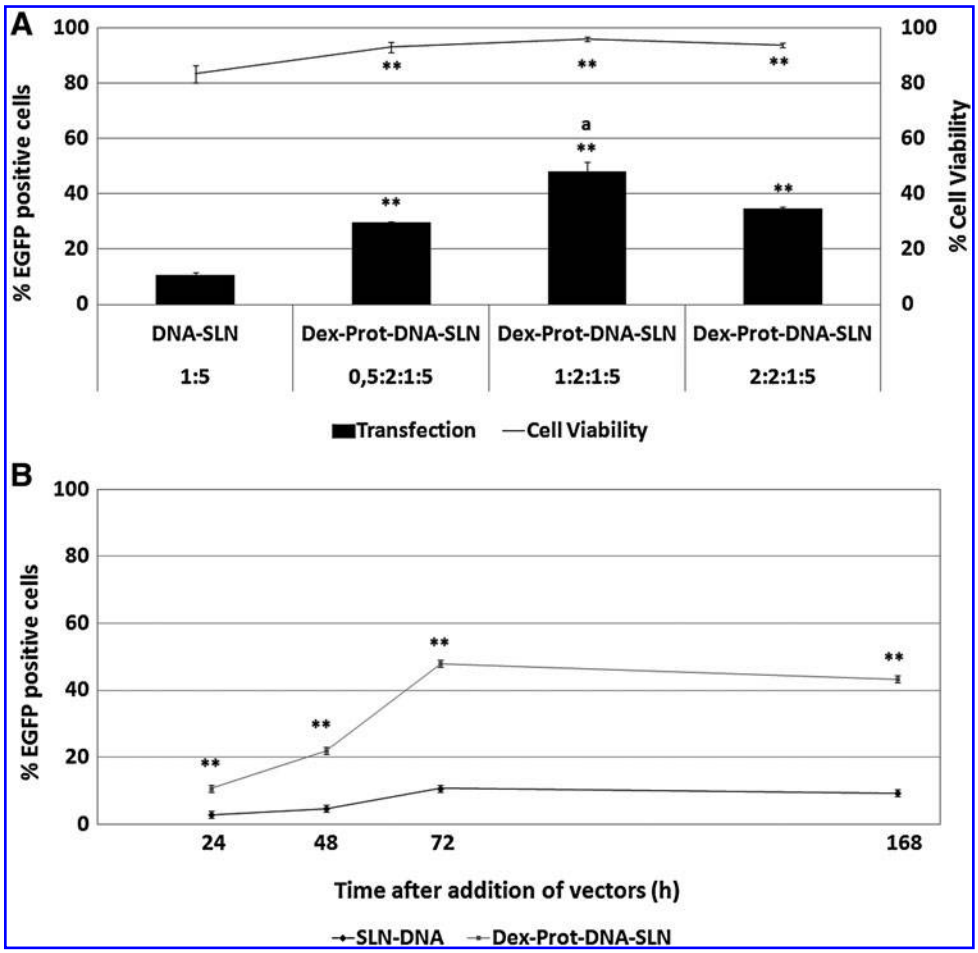

FIG. 4. (A) Transfection (columns) and cell viability (line) for each formulation assayed in ARPE-19 cells at 72 hr; the SLN-to-DNA ratio (w/w) was 5:1 in all cases, and the dextran–protamine–DNA ratio varied from 0.5:2:1 to 2:2:1. **(B)** Transfection of ARPE-19 cells by nonviral vectors over time. The SLN-to-DNA ratio (w/w) was 5:1 and the dextran–protamine–DNA–SLN ratio was 1:2:1:5. Error bars represent the SD ($n=3$). $^{**}p<0.01$ with respect to the DNA–SLN formulation. $^{a}p<0.01$ with respect to all other formulations.

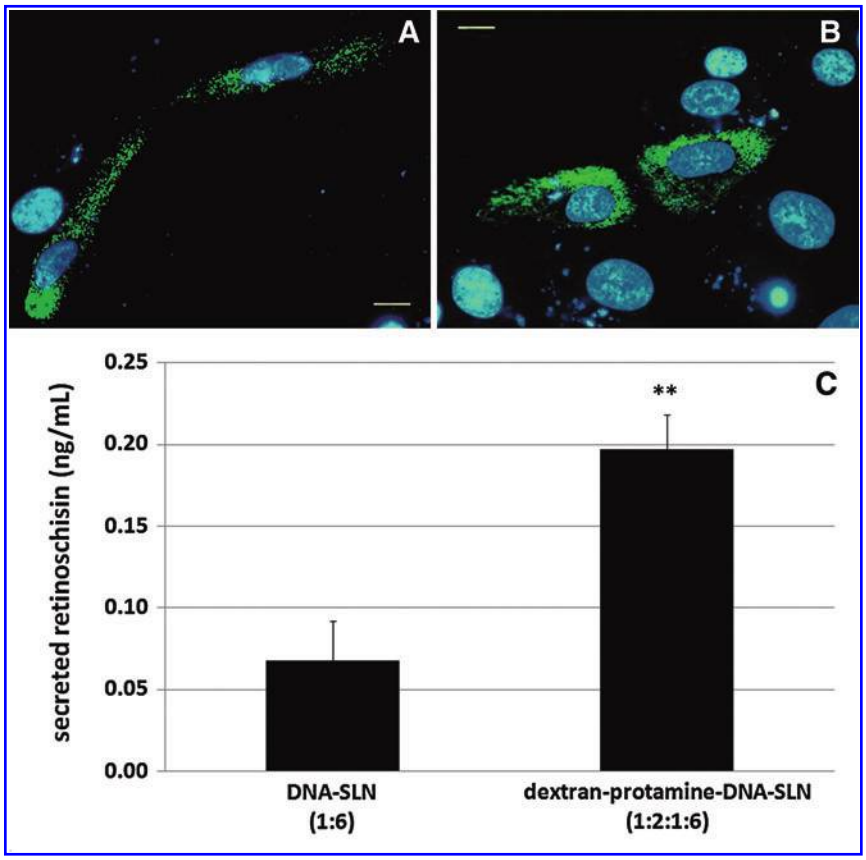

FIG. 5. Detection of retinoschisin expressed in ARPE-19 cells by fluorescence microscopy after transfection with **(A)** dextran–protamine–DNA–SLN vector (1:2:1:6) and **(B)** DNA–SLN vector (1:6). **(C)** Quantification of secreted retinoschisin. Green, retinoschisin labeled with Alexa Fluor 488; Blue, DAPI nuclear stain. Scale bar: 50 μm. $^{**}p<0.01$ with respect to DNA–SLN vector. Color images available online at www.liebertonline.com/hum

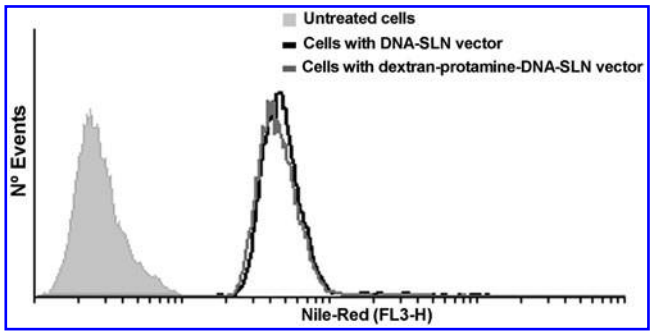

FIG. 6. Flow cytometric analysis of cellular uptake of DNA–SLN vector and dextran–protamine–DNA–SLN vector by ARPE-19 cells. Vectors were labeled with Nile red.

containing protamine and dextran was added to the cells (yellow color in Fig. 7D). This result is confirmed by the Manders overlap coefficient (Table 1); the highest value of this coefficient (0.78) was achieved with the dextran–protamine–DNA–SLN formulation and transferrin (values close to 1 indicate high colocalization). Figure 7E shows higher magnifications of Fig. 7C and D, featuring colocalization between the vector and the clathrin marker and the lack of colocalization with the caveola marker. These results indicate that when dextran and protamine are added to SLNs, endocytosis via clathrin is the predominant mechanism of cell internalization.

Protein expression after ocular administration

To explore the *in vivo* potential of the developed SLN complexes in ocular gene therapy, dextran–protamine–DNA–SLN vectors were loaded with plasmid encoding enhanced green fluorescent protein (pCMS-EGFP) and injected into the retina by various administration routes. Our data show that pCMS-EGFP can be successfully delivered and expressed in the eye (Fig. 8). The level of expression in the eye varied depending on the location of the intraocular injection. Thus, after intravitreal injection, high levels of gene expression were found mainly at the retinal ganglion cells (Fig. 8A and 8B). Only modest expression was found in the remaining layers of the retina and little expression was detected in the retinal pigment epithelium (RPE). In contrast, after subretinal injection, expression was substantially higher in the RPE layer (Fig. 8C and 8D). Furthermore, we also found some expression in photoreceptors and the outer nuclear layer.

To further assess the *in vivo* efficacy of dextran–protamine–DNA–SLN complexes for the delivery of nucleic acids into ocular tissue, a solution of the complexes was instilled onto rat corneas. Gene expression was visible 72 hr postadministration (Fig. 9). Taken together, the vectors were able to interact with corneal cells and penetrate through the corneal epithelium. EGFP expression lasted at least 5 days and was located mainly inside the cells, suggesting a transcellular mechanism of transport.

No green fluorescence was detected in the samples from rats treated with vectors without plasmid. Evidence of toxicity was not detected in the animals, irrespective of the formulation administered.

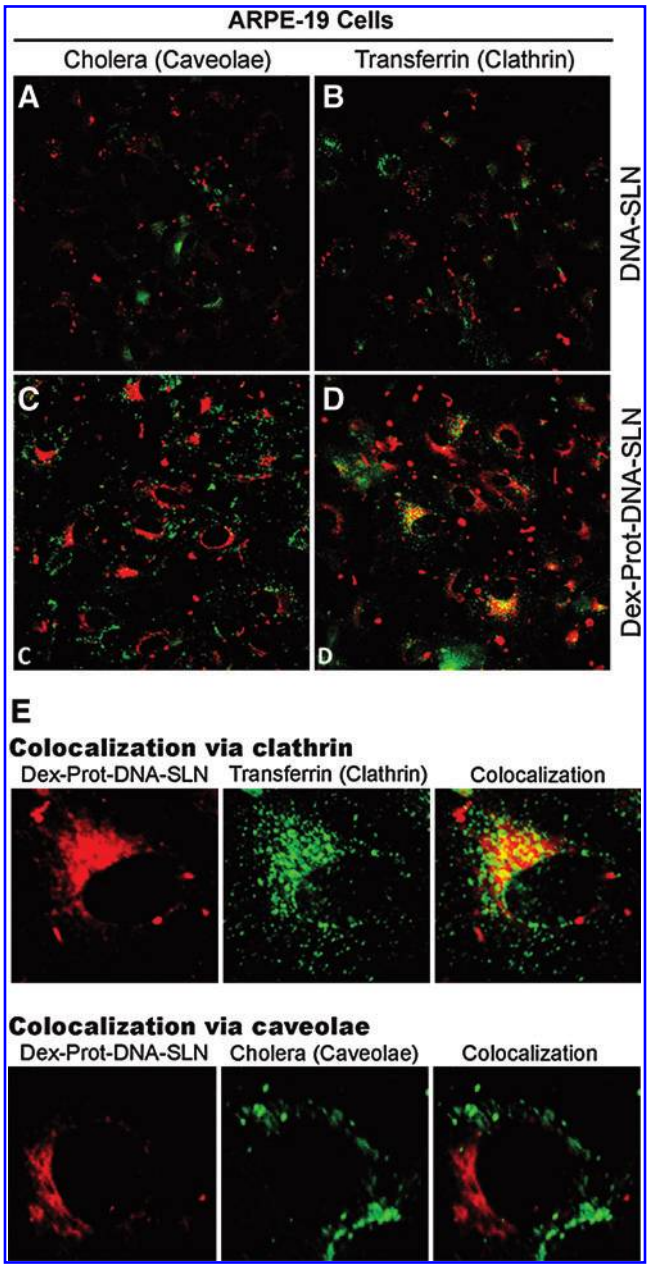

FIG. 7. Confocal laser scanning microscopy images of Nile red-labeled DNA–SLN and dextran–protamine–DNA–SLN vectors in ARPE-19 cells with Alexa Fluor 488–cholera toxin (green) at 10 μg/ml **(A** and **C)**; or with Alexa Fluor 488–transferrin (green) at 50 μg/ml **(B** and **D)**. The SLN-to-DNA ratio (w/w) was 5:1 and the dextran–protamine–DNA–SLN ratio was 1:2:1:5 **(E)**. Color images available online at www.liebertonline.com/hum

Discussion

In spite of advances in the field of viral gene therapy for the treatment of degenerative ocular diseases, a safe and highly efficient alternative delivery system is still needed. Therapy with viral vectors improved the visual function in patients with Leber's congenital amaurosis (Bainbridge *et al.*, 2008; Maguire *et al.*, 2009). Nevertheless, safety concerns and the availability of suitable viral vectors limit their clinical application. Nonviral vectors are a promising

Table 1. Coefficients of Colocalization Analysis in ARPE-19 Cells

	Endocytosis via caveolae		*Endocytosis via clathrin*	
	DNA–SLN	*Dex–Prot–DNA–SLN*	*DNA–SLN*	*Dex–Prot–DNA–SLN*
R	0.535 ± 0.174	0.378 ± 0.037	0.424 ± 0.124	0.780 ± 0.050

Dex, dextran; Prot, protamine; *R*, Manders overlap coefficient (values from 1 to 0; values more than 0.6 indicates high colocalization); SLN, solid lipid nanoparticles.

alternative to viral vectors because of a more favorable safety profile, although additional work is required to improve their efficacy.

In this paper, we have shown for the first time the *in vivo* capacity of solid lipid nanoparticles to transfect ocular tissues after administration to the rat eye (Conley and Naash, 2010). In previous work we had already demonstrated the usefulness of protamine to promote *in vitro* transfection of ARPE-19 cells with solid lipid nanoparticles (Delgado *et al.*, 2011). Protamine is a small peptide (MW, 4,000–4,250) that efficiently condenses DNA. This facilitates the control of formulation processes, prevents the formation of aggregates, and contributes to protection against DNase degradation (Ye *et al.*, 2008). Moreover, protamine presents nuclear localization signal (NLS) sequences with high arginine content and, thus, enhances DNA entry into the nucleus (Sorgi *et al.*, 1997; Ye *et al.*, 2008). Besides protamine, the present study has also incorporated dextran into the solid lipid nanoparticles. This polyanion-biocompatible polysaccharide hampers strong interactions with other components such as serum proteins (Maruyama *et al.*, 2004) that could have an influence on transfection, especially *in vivo* (Finsinger *et al.*, 2000). Furthermore, dextrans are typically used as clathrin-mediated endocytosis markers. Theoretically, the ability of dextran to enhance cellular uptake by the endolysosomal pathway (Agarwal *et al.*, 2009) needs to be considered because we have previously demonstrated that protamine works most efficiently when clathrins are involved in the entry mechanism of vectors (Delgado *et al.*, 2011).

The presence of protamine and dextran in the complex modified neither the particle size nor the surface charge of the solid lipid nanoparticles. The complexes we prepared were able to protect the genetic material from DNases and to release the DNA in the presence of SDS. Because pCEP4-RS1 has a higher molecular mass (11.1 kb) than pCMS-EGFP (5.5 kb), a higher DNA-to-SLN ratio was necessary for pCEP4-RS1 than for pCMS-EGFP to maintain the capacity to protect the genetic material without affecting the ability to release DNA (1:5 vs. 1:6 ratio). This optimization is important for gene therapy applications, as excessive DNA condensation impedes plasmid release and transfection. In contrast, low condensation will not protect DNA inside the cells (del Pozo-Rodríguez *et al.*, 2007).

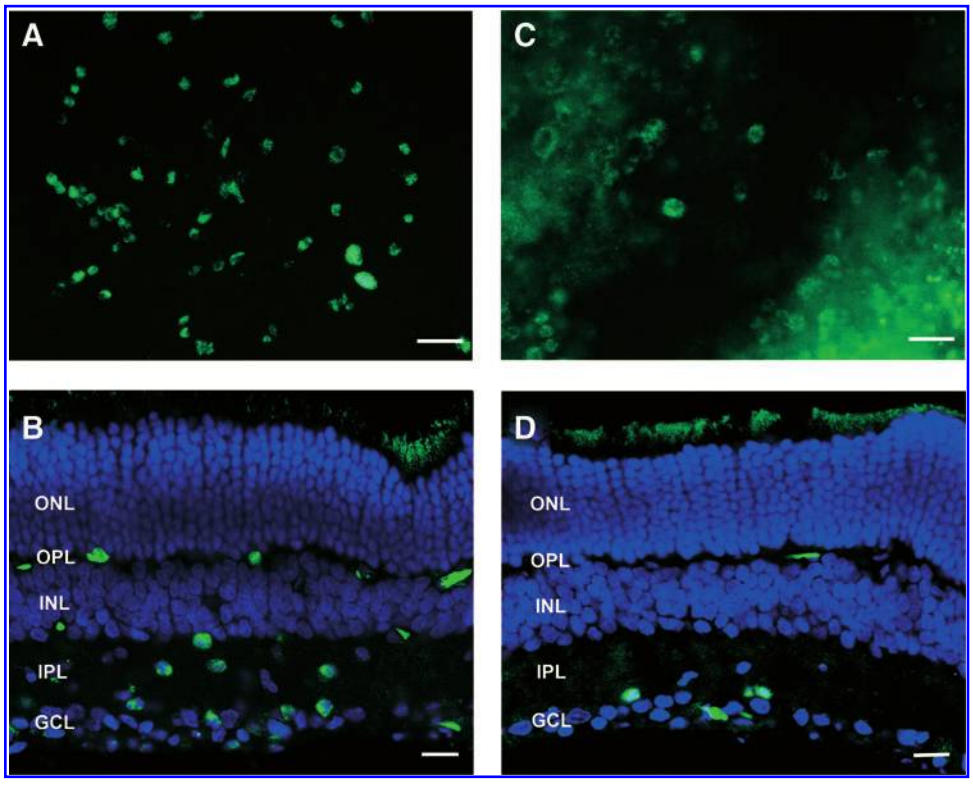

FIG. 8. pCMS-EGFP expression in the retina 72 hr after transfection with dextran–protamine–DNA–SLN vector. **(A** and **C)** Whole-mount retinas. **(B** and **D)** Cryostat sections with cell nuclei counterstained with Hoechst (blue). Note the prominent localization of pCMS-EGFP in the inner retinal layers after a single intravitreal injection **(A** and **B)**, whereas with subretinal injection the transfection can be seen in several layers, primarily in the retinal pigment epithelium and photoreceptors but also in processes at the outer plexiform layer and in some retinal ganglion cells **(C** and **D)**. ONL, outer nuclear layer; OPL, outer plexiform layer; INL, inner nuclear layer; IPL, inner plexiform layer; GCL, ganglion cell layer. Scale bars: 25 μm. Color images available online at www.liebertonline.com/hum

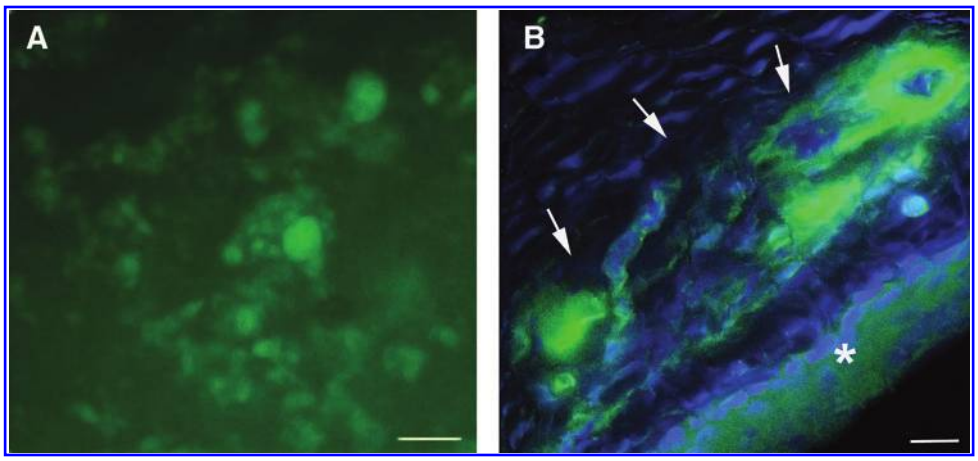

FIG. 9. pCMS-EGFP expression in the cornea after topical administration of dextran–protamine–DNA–SLN vector. **(A)** Fluorescence micrograph of a whole-mount cornea prepared 72 hr after instillation. **(B)** Confocal micrograph of a cryostat section of the cornea 72 hr postinstillation. Cell nuclei were counterstained with Hoechst (blue). Asterisk shows the corneal epithelium. Arrows indicate the corneal stroma. Scale bars: 50 μm. Color images available online at www.liebertonline.com/hum

Transfection studies with vectors containing pCMS-EGFP plasmid showed that the presence of protamine and dextran significantly increased the transfection capacity of the SLNs (Fig. 4). The most efficient formulation was prepared with a dextran–protamine–DNA ratio of 1:2:1. Our data point to the importance of adequately optimizing the proportion of additives to prepare safe and efficient formulations. It is important to highlight the high transfection level obtained, close to 50% of cells transfected. This is even more intriguing because ARPE-19 cells are difficult to transfect. For example, Abul-Hassan and colleagues reported 25% transfection efficiency for this cell line and other authors achieved even lower transfection rates (Abul-Hassan *et al.*, 2000; Bejjani *et al.*, 2005). In previous studies we achieved transfection levels close to 30% when SLNs were combined with protamine (Delgado *et al.*, 2011); these levels have been significantly increased in this work by adding dextran to that formulation.

To confirm the usefulness of the vectors for XLRS treatment, we prepared formulations in which the model pCMS-EGFP plasmid was replaced with a therapeutic plasmid, pCEP4-RS1. Both plasmids were assayed for their transfection capacity in ARPE-19 cells. Retinoschisin, the encoded protein, is an extracellular protein secreted by photoreceptors and bipolar cells that is involved in retinal organization and stability (Molday *et al.*, 2001). After transfection, we detected cytoplasmic retinoschisin by immunochemistry, and we also quantified the secreted retinoschisin (Fig. 5). Fluorescence microscopy images show that the vectors we prepared (SLNs with and without protamine and dextran) were able to produce retinoschisin. Moreover, the amount of protein secreted was higher when the cells were transfected with the formulation containing protamine and dextran. These results are in line with the transfection results of pCMS-EGFP.

While designing and optimizing a vector for gene therapy, the knowledge of entry mechanisms and intracellular trafficking is useful, because these limiting steps may be modulated by the formulation. In a previous study (Delgado *et al.*, 2011), we observed that clathrin-mediated endocytosis is needed to achieve transfection when vectors bear protamine. As mentioned previously, one of the reasons for the addition of dextran to our vector is the common use of dextrans as clathrin and endolysosomal markers. As expected, the presence of dextran induced higher internalization of dextran–protamine–DNA–SLN vectors via clathrin, which promoted a rise in transfection levels (Fig. 7). Therefore, our previous observations have been confirmed here; indeed, the higher the entry via clathrin, the higher the transfection achieved with vectors bearing protamine.

We carried out a further preliminary *in vivo* study to assess whether the vectors are able to transfect ocular tissues after their administration by various ocular routes: intravitreous, subretinal, and topical. In animal models, an *in vitro–in vivo* correlation is not necessarily expected, because of possible physical barriers (Peeters *et al.*, 2005; de la Fuente *et al.*, 2010).

After ocular administration of dextran–protamine–DNA–SLN complex to rat eyes, we detected the expression of green fluorescent protein in various types of cells depending on the administration route. There was a good response in retinal ganglion cells when intravitreal injection was employed, but protein expression was poor in RPE cells (Fig. 8A and 8B). In contrast, after subretinal injection, the vectors were able to transfect RPE cells as well as photoreceptors (Fig. 8C and 8D). These results are in line with those obtained in a previous study in which intravitreous administration of adenoviral vectors induced protein expression in the inner retina, whereas RPE cells and outer retina were the cells primarily transfected after subretinal administration (Colella *et al.*, 2009). This preliminary study may be useful to select the target cells to be transfected depending on the target of gene therapy. Nonviral vectors could be employed to treat various diseases such as glaucoma when the inner retina needs to be addressed, or retinoschisis and retinitis pigmentosa, if administration reaches the outer retina (Phelan and Bok, 2000; Johnson *et al.*, 2009).

Our vectors were also able to transfect corneal cells after topical application (Fig. 9). As this route of administration is noninvasive, and corneal immune defense does not induce inflammation, these vectors may be safe for the treatment of corneal endothelial dystrophies and to modulate protein production in order to control the corneal microenvironment (Klausner *et al.*, 2007).

Therefore, we have demonstrated the potential usefulness of solid lipid nanoparticle-based nonviral vectors loading XLRS1 plasmid in the treatment of X-linked juvenile retinoschisis. Taking into account that the transfection process depends on plasmid size, this type of vector may be useful to load other therapeutic plasmids with a molecular size similar to that of XLRS1. Taken together, we have provided evidence for the potential application of dextran–protamine–DNA–SLN vectors for the treatment of degenerative retinal disorders as well as ocular surface diseases.

Acknowledgments

This research was supported by grants from the University of the Basque Country UPV/EHU to D.D. (PIFA01/20067008); by the Basque Government's Department of Education, Universities and Investigation (IT-341-10); by grants from the Spanish Ministry of Education and Science (SAF2010-19862, SAF2008-03694), the ONCE (National Organization of the Spanish Blind), and the Bidons Egara Research Chair in Retinosis Pigmentosa to E.F.; and by grants from the Deutsche Forschungsgemeinschaft (DFG) to B.H.F.W. (WE1259/12-4). The authors also acknowledge the General Service of Analytical Microscopy and High Resolution in Biomedicine of the University of the Basque Country UPV/EHU for technical advice on confocal microscopy and A.R. Díaz for valuable participation in the experiments; and D. Gonzalez for technical assistance.

Author Disclosure Statement

No competing financial interests exist.

References

Abul-Hassan, K., Walmsley, R., and Boulton, M. (2000). Optimization of non-viral gene transfer to human primary retinal pigment epithelial cells. Curr. Eye Res. 20, 361–366.

Agarwal, A., Gupta, U., Asthana, A., and Jain, N.K. (2009). Dextran conjugated dendritic nanoconstructs as potential vectors for anti-cancer agent. Biomaterials 30, 3588–3596.

Bainbridge, J.W., Smith, A.J., Barker, S.S., *et al*. (2008). Effect of gene therapy on visual function in Leber's congenital amaurosis. N. Engl. J. Med. 358, 2231–2239.

Bejjani, R.A., BenEzra, D., Cohen H., *et al*. (2005). Nanoparticles for gene delivery to retinal pigment epithelial cells. Mol. Vis. 17, 124–132.

Bloquel, C., Bourges, J.L., Touchard, E., *et al*. (2006). Non-viral ocular gene therapy: Potential ocular therapeutic avenues. Adv. Drug Deliv. Rev. 58, 1224–1242.

Colella, P., Cotugno, G., and Auricchio, A. (2009). Ocular gene therapy: Current progress and future prospects. Trends Mol. Med. 15, 23–31.

Conley, S.M., and Naash, M.I. (2010). Nanoparticles for retinal gene therapy. Prog. Retin. Eye Res. 29, 376–397.

de la Fuente, M., Raviña, M., Paolicelli, P., *et al*. (2010). Chitosan-based nanostructures: A delivery platform for ocular therapeutics. Adv. Drug Deliv. Rev. 62, 100–117.

Delgado, D., del Pozo-Rodríguez, A., Solinís, M.A., and Gascón, A.R. (2011). Understanding the mechanism of protamine in solid lipid nanoparticle-based lipofection: The importance of the entry pathway. Eur. J. Pharm. Biopharm. 79, 495–502.

del Pozo-Rodríguez, A., Delgado, D., Solinís, M.A., *et al*. (2007). Solid lipid nanoparticles: Formulation factors affecting cell transfection capacity. Int. J. Pharm. 339, 261–268.

del Pozo-Rodríguez, A., Delgado, D., Solinís, M.A., *et al*. (2008). Solid lipid nanoparticles for retinal gene therapy: Transfection and intracellular trafficking in RPE cells. Int. J. Pharm. 360, 177–183.

del Pozo-Rodriguez, A., Pujals, S., Delgado, D., *et al*. (2009). A proline-rich peptide improves cell transfection of solid lipid nanoparticles-based non-viral vectors. J. Control. Release 133, 52–59.

Finsinger, D., Remy, J.S., Erbacher, P., *et al*. (2000). Protective copolymer for nonviral gene vectors: Synthesis, vector characterization and application in gene delivery. Gene Ther. 7, 1183–1192.

Gascón, A.R., Solinís, M.A., del Pozo-Rodríguez, A., *et al.* (2011). Lipid nanoparticles for gene therapy. WO2011015701.

Hamel, C. (2006). Retinitis pigmentosa. Orphanet J. Rare Dis. 1, 40.

Janssen, A., Min, S.H., Molday, L.L., *et al.* (2008). Effect of late-stage therapy on disease progression in AAV-mediated rescue of photoreceptor cells in the retinoschisin-deficient mouse. Mol. Ther. 16, 1010–1017.

Jiang, C., Moore, M.J., Zhang, X., *et al*. (2007). Intravitreal injections of GDNF-loaded biodegradable microspheres are neuroprotective in a rat model of glaucoma. Mol. Vis. 13, 1783–1792.

Johnson, E.C., Guo, Y., Cepurna, W.O., and Morrison, J.C. (2009). Neurotrophin roles in retinal ganglion cell survival: Lessons from rat glaucoma models. Exp. Eye Res. 88, 808–815.

Klausner, E.A., Peer, D., Chapman, R.L., *et al*. (2007). Corneal gene therapy. J. Control. Release 124, 107–133.

Kumar-Singh, R. (2008). Barriers for retinal gene therapy: Separating fact from fiction. Vision Res. 48, 1671–1680.

Liu, X., Brandt, C.R., Rasmussen, C.A., *et al*. (2007). Ocular drug delivery: Molecules, cells and gene. Can. J. Ophthalmol. 42, 447–454.

Maguire, A.M., High, K.A., Auricchio, A., *et al.* (2009). Age-dependent effects of RPE65 gene therapy for Leber's congenital amaurosis: A phase 1 dose-escalation trial. Lancet 374, 1597–1605.

Maruyama, K., Iwasaki, F., Takizawa, T., *et al*. (2004). Novel receptor-mediated gene delivery system comprising plasmid/protamine/sugar-containing polyanion ternary complex. Biomaterials 25, 3267–3273.

Min, S.H., Molday, L.L., Seeliger, M.W., *et al*. (2005). Prolonged recovery of retinal structure/function after gene therapy in an Rs1h-deficient mouse model of X-linked juvenile retinoschisis. Mol. Ther. 12, 644–651

Molday, L.L., Hicks, D., Sauer, C.G., *et al*. (2001). Expression of X-linked retinoschisis protein RS1 in photoreceptor and bipolar cells. Invest. Ophtalmol. Vis. Sci. 42, 816–825.

Mooy, C.M., Van Den Born, L.I., Baarsma, S., *et al.* (2002). Hereditary X-linked juvenile retinoschisis: A review of the role of Müller cells. Arch. Ophthalmol. 120, 979–984.

Naik, R., Mukhopadhyay, A., and Ganguli, M. (2009). Gene delivery to the retina: Focus on non-viral approaches. Drug Discov. Today 14, 306–315.

Nour, M., Quiambao, A.B., Peterson, W.M., *et al*. (2003). $P2Y_2$ receptor agonist INS37217 enhances functional recovery after detachment caused by subretinal injection in normal and *rds* mice. Invest. Ophthalmol. Vis. Sci. 44, 4505–4514.

Peeters, L., Sanders, N.N., Braeckmans, K., *et al*. (2005). Vitreous: A barrier to nonviral ocular gene therapy. Invest. Ophthalmol. Vis. Sci. 46, 3553–3561.

Phelan, J.K., and Bok, D. (2000). A brief review of retinitis pigmentosa and the identified retinitis pigmentosa gene. Mol. Vis. 8, 116–124.

Provost, N., Le Meur, G., Weber, M., *et al*. (2005). Biodistribution of rAAV vectors following intraocular administration: Evidence for the presence and persistence of vector DNA in the optic nerve and in the brain. Mol. Ther. 11, 275–283.

Sorgi, F.L., Bhattcharya, S., and Huang, L. (1997). Protamine sulfate enhances lipid-mediated gene transfer. Gene Ther. 4, 961–968.

Ye, J., Wang, A., Liu, C., *et al*. (2008). Anionic solid lipid nanoparticles supported on protamine/DNA complexes. Nanotechnology 19, 285708.

Zinchuk, V., and Zinchuk, O. (2008). Quantitative colocalization analysis of confocal fluorescence microscopy images. Curr. Protoc. Cell Biol. 39, 4.19.1–4.19.16.

Address correspondence to:
Dr. Alicia Rodríguez Gascón
Pharmacokinetics, Nanotechnology and Gene Therapy Group
Laboratory of Pharmacy and Pharmaceutical Technology
Pharmacy Faculty
University of the Basque Country UPV/EHU
Paseo de la Universidad 7
01006 Vitoria-Gasteiz
Spain

E-mail: alicia.rodriguez@ehu.es

Received for publication July 3, 2011;
accepted after revision January 27, 2012.

Published online: February 1, 2012.